ARCHIVES of FOUNDRY ENGINEERING

Published quarterly as the organ of the Foundry Commission of the Polish Academy of Sciences

ISSN (1897-3310)
Volume 14
Special Issue
1/2014
131-134

26/1

Analysis of the Content of δ Ferrite in Pulse-Arc Welded Steel 304

M. Gucwa [a]*, R. Bęczkowski [a], A. Grzyb [a]

[a] Department of Welding Technology, Czestochowa University of Technology, 69 J.H. Dąbrowskiego St., 42-201 Czestochowa, Poland

* Corresponding author's e-mail: mgucwa@spaw.pcz.pl

Received on 17.03.2014; accepted in revised form 31.03.2014

Abstract

The paper presents the results of research on the effect of the welding arc type on the content of δ ferrite, in the welded joint of 304 grade stainless steel. Based on the commonly used Schaefler diagram, the content of δ ferrite in the welded joint was estimated, and then these results were verified by comparing them with results obtained on specimens welded by different welding arc types, including the pulse arc. The obtained investigation results indicate some discrepancies between calculations made by analytical methods and the fraction of δ ferrite measured on the prepared specimens.

Keywords: Stainless steel ,δ ferrite, Welding arc, Schaefler diagram,

1. Introduction

Austenitic stainless steels normally have an austenitic matrix with a varying content of δ ferrite. When the amount of δ ferrite is too low (below 5%), hot cracks can occur during welding. An excessive amount of δ ferrite (above 10%) causes a reduction in ductility, hardness and corrosion resistance in austenitic weldable stainless steels. It should be borne in mind that the presence of δ ferrite in the structure of an austenitic weld, in the temperature range of 600÷900°C, may cause the formation of an intermetallic compound of chromium and iron called the sigma (σ) phase. The sigma phase contains 40÷60% chromium, approx. 30% iron and slight amounts of nickel and molybdenum. This phase reduces the plastic properties and impact resistance of weld metal, and also impairs the corrosion resistance of stainless steels [1,2]. In the case of heterogeneous joints, a significant increase of hardness in the weld is observed, as compared both to the heat-affected zone and the parent material [3]. The formation of the σ phase due to welding is prevented by:

- using low linear energies during welding and additional cooling of the joint,
- overcooling the welded elements and avoiding their reheating up to temperatures in the range from 600 to 900°C,
- using filler metals of enhanced contents of austenite-forming additions, particularly nickel, for welding [4].

Besides the chemical composition, the amount of δ ferrite in the structure is influenced also by the technology of production of a particular steel grade, while in the case of welds, the welding technology, whose effect can be expresses by the rate of heat removal from the welding puddle. Depending on the current–voltage parameters, welding speed and the welded element's thickness and temperature, the rate of heat removal from the weld zone is varied. The increase in heat removal rate for duplex steels causes the amount of δ ferrite in the structure to increase. In turn, in the case of austenitic and austenitic–ferritic steels, the fraction of ferrite in the structure grows up to a certain cooling rate and then it falls [5,6]. For the analysis of the amount of ferrite in stainless steels, Schaeffler diagrams and WWRC-1992 are normally used [7]. However, these diagrams do not consider the

technological parameters of the welding process, but only the chemical composition of basic materials and fillers.

2. Materials and research methods

The purpose of the study is to investigate the effect of the mode of metal transfer in the welding arc and of the pulse arc on the content of δ ferrite in the welded joint of stainless steel. The subject of investigation were fillet-weld tee joints welded by the MIG method. For all specimens, 4 mm-thick AISI 304 plates steel was used, while as a filler to be tested, 1 mm-gauge „Starweld 316LSi" wire was used. The welding stand was equipped with an Ozas Synermig 400 semi-automatic welder with a ZP-25 feeder. For the tests, 300x60mm sheets were used, from which specimens 1A, 2A, 3A, 4A were subsequently made to be welded with different modes of metal transfer in the arc, and 200x40mm sheets, out of which specimens 1B, 2B ,3B were prepared to be welded with pulse current. The table 1 lists welding parameters along with the designations of specimens.

Table 1.
Welding process parameters

Specimen No.	Current [A]	Voltage [V]	Arc type	Frequency [Hz]
1A	150	20.1	Shorting	
2A	167	23.2	Mixed	
3A	207	30.0	Spray	
4A	258	36.6	Spray	
1B	165	28.2	Pulse	155
2B	150	26.8	Pulse	141
3B	180	29.8	Pulse	169

The next investigation stage involved the preparation of metallographic microsections and the measurement of the content of δ ferrite in the welded joint. The δ ferrite content was measured with a „Helmut Fischer GMBH+CO" ferrite meter, type FE8d3. On each microsection area examined (Fig. 1), 2–5 measurements were taken, and the results were averaged. For the calculations of estimated δ ferrite contents, the Schaeffler diagram was used, in which the calculated coefficients for the weld and the parent material were indicated.

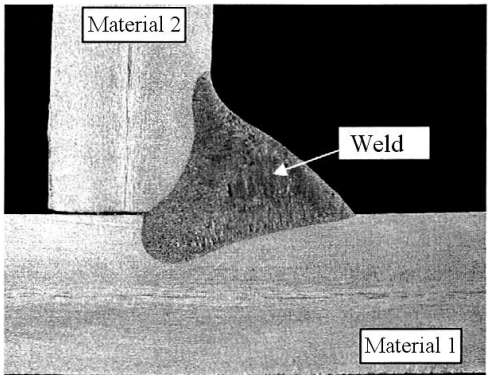

Fig. 1. Denotations of respective joint zones, which were used for the determination of the δ ferrite content

3. Investigation results and their analysis.

Table 2 summarizes the results of measurements of the content of δ ferrite in the welded joints and the content of δ ferrite in the weld calculated using the Schaeffler diagram.

Table 2
The content of δ ferrite in the welded joint

Specimen No.	Ferrite meter measurement [%]			Schaeffler diagram data [%}
	Material 1	Material 2	Weld	
1A	0.1	1.2	4.8	
2A	0.6	0.8	5.2	
3A	0.2	1.2	5.6	
4A	0.5	0.9	7.4	10
1B	0.3	0.6	5.2	
2B	0.2	0.4	6.2	
3B	0.9	0.3	7.0	

.

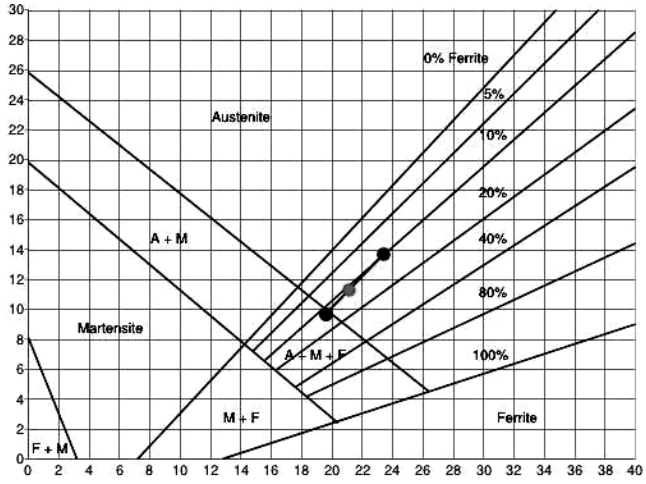

Fig. 2. Schaeffler diagram with the indicated fraction of δ ferrite in the structure [7]

The content of δ ferrite measured on the joints made deviate from those obtained by calculations and the analysis of the Schaeffer diagram. This is caused by the interaction of the welding arc and the non-equilibrium conditions of weld crystallization. This is particularly clearly visible for the analysis of the δ ferrite fraction of the parent material structure. Figure 2 suggests that the δ ferrite fraction of the parent material structure should be similar to that noted in the weld. The examination using the ferrite meter indicate a much lower ferrite fraction of the weld, as also corroborated by microscopic observations. In fig. 3-8, several examples of microstructures observed on the prepared metallographic microsections are displayed. All the presented microstructures were prepared by electrolytic etching.

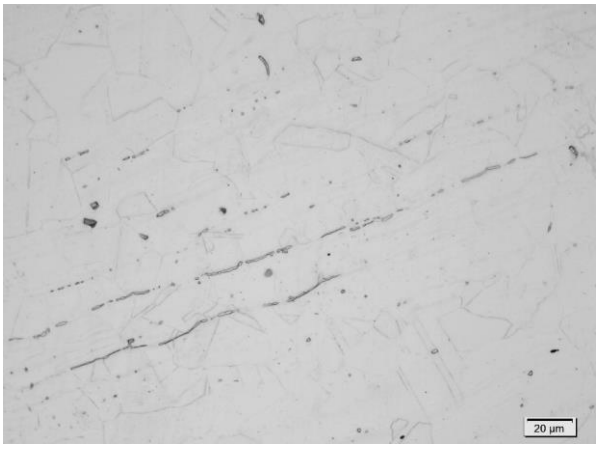

Fig. 3. Microstructure of the parent material, magnification of 500x.

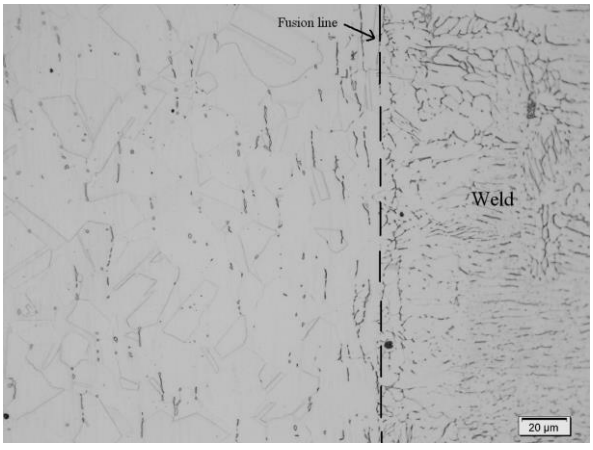

Fig. 4. Microstructure of specimen 2A, magnification of 500x.. The line of fusion is visible

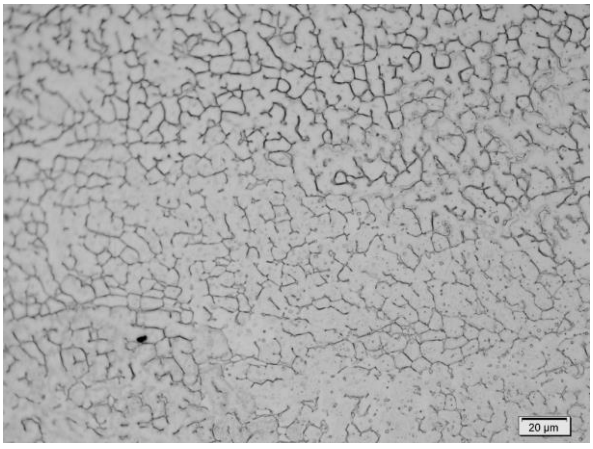

Fig. 5. Microstructure of specimen 1A, magnification of 500x. The weld is visible

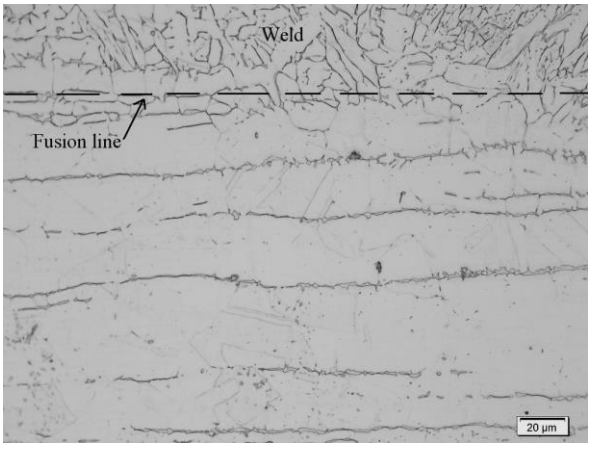

Fig. 6. Microstructure of specimen 1B, magnification of 500x. The line of fusion is visible

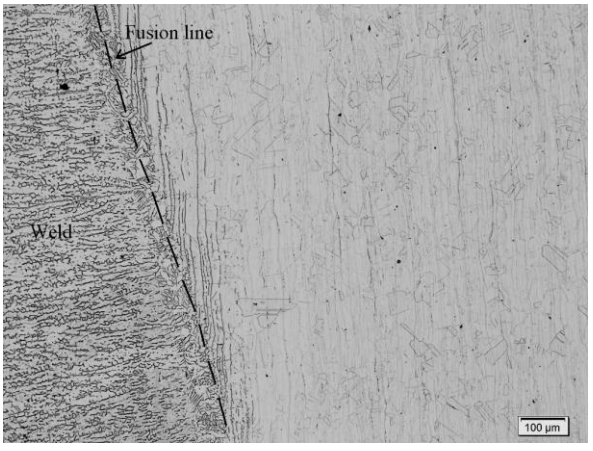

Fig. 7. Microstructure of specimen 3B, magnification of 100x. The line of fusion is visible

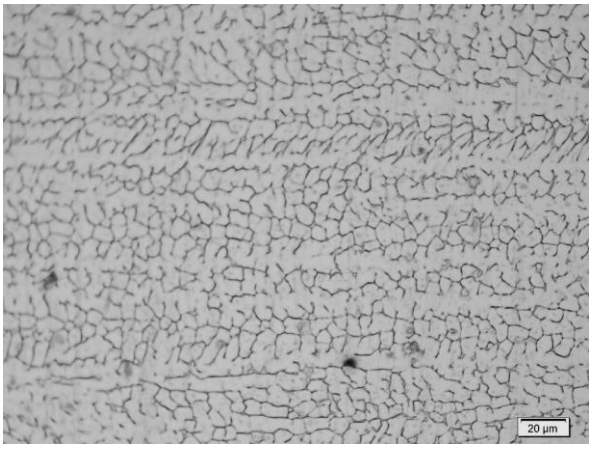

Fig. 8. Microstructure of specimen 2B, magnification of 500x. The weld is visible

The analysis of the welds made using, respectively, pulse and non-pulse welding, has not shown any significant differences in microstructure. In each of the welded joints made, an increase in the content of δ ferrite with the increase in the magnitude of welding current intensity can be noticed. In spite of lower current intensity magnitudes for pulse welding, no significant differences in the amount of δ ferrite formed in the structure have been noted. This is due to the properties of pulse welding, for which the magnitude of pulse current intensity should have considered, which is higher than the average value given in Table 1.

In the microstructure image displayed (Fig. 3), lamellar δ ferrite precipitates are visible in the austenitic matrix. The quantity of ferrite is small and correlates with the results obtained from the examination of the ferrite content with a ferrite meter. In the region of the line of fusion (Figs. 4, 6 and 7), an increased content of δ ferrite is visible, which is due to the parent material being mixed with the weld metal. The high welded joint cooling rates have caused some quantity of unconverted δ ferrite to remain in the weld and in the line-of-fusion region, which may undergo transformation into austenite under slow cooling conditions. In addition, segregation occurring in the solidification process and the material mixing have the effect of slowing down the rate of δ ferrite transformation into austenite.

The welding arc thermal power, which is the product of welding current intensity times welding voltage, differs considerably between standard welding and pulse welding. In the examined cases for joints denoted as 4A and 3B, the thermal power of the pulse arc was lower by 44%. In spite of this, the amount of δ ferrite contained in the weld is on a similar level. So, there is the issue of correct estimation of the amount of heat supplied to the joint.

4. Conclusions

Based on the obtained research results, the following conclusions can be drawn.

1. Using pulse welding did not reduce the content of δ ferrite contained in the welded joint structure compared to non-pulse welding. In the cases under examination, the thermal conditions were similar for each of the welds made.
2. Frequency changes in pulse welding have an effect on the content of δ ferrite by changing the quantity and size of the drops of liquid metal transferred within the electric arc, and thus changing the thermal conditions of welded joint cooling.
3. The thermal power of the pulse arc is not estimated correctly in the literature [4]. This is due to reducing the calculations to the averaged values of current and voltage only, while omitting the dynamic changes of the arc parameters.

References

[1] Brodziak-Hyska A., Stradomski Z., Kolan C.(2014) Kinetics of the σ phase precipitation in respect of erosion–corrosion wear of duplex cast steel. *Archive of Foundry*.14,17-20

[2] Stradomski Z., Brodziak-Hyska A., Kolan C. (2012) Optimization of sigma phase precipitates with respect to the functional properties of duplex cast steel. *Archive of Foundry*.12,75-78

[3] Khalifeh A.R.,Dehghan A.,Hajjari E. (2013). Dissimilar Joining of AISI 304L/St37 Steels by TIG Welding Process.*Acta Metallurgica Sinica*. 26,*721-727*

[4] Hsieh C.C., Lin D.Y., Chen M.C., Wu W. (2008) Precipitation and strengthening behavior of massive δ-ferrite in dissimilar stainless steels during massive phase transformation. *Materials Science and Engineering A.* 477, 328–333.

[5] Pilarczyk J. et al., (2003) *Handbook for engineers Volume 1 – Welding.* Warsaw WNT

[6] Dyja. D, Stradomski Z. (2007). Optimization of heat treatment in aspect of production's costs reducing and improving of casting quality from duplex cast steel. *Archive of Foundry*.7,39-42

[7] Vitek M., David S. A., Hinman C. R.. (2003) Improved Ferrite Number Prediction Model that Accounts for Cooling Rate Effects — Part 1: Model Development. *Welding Journal*. 10-17

[8] Sudhakaran R., VeL Murugan V., Sivasakthivel P. S., Balaji M. (2013). Modeling and analysis of ferrite number of stainless steel gas tungsten arc welded plates using response surface methodology. *International Journal of Advanced Manufacturing Technology*. 64,1487-1504

[9] Tasak E. (2008). *Welding Metallurgy.* Krakow: JAK Publishers